Proceedings of the ASME 2022 Conference on Smart Materials,
Adaptive Structures and Intelligent Systems
SMASIS2022
September 12-14, 2022, Dearborn, MI

SMASIS2022-91587

IMPLICATIONS OF RESISTIVE FORCE ON VARIABLE RECRUITMENT FLUIDIC ARTIFICIAL MUSCLE BUNDLE STATE TRANSITION

Jeong Yong Kim
North Carolina State University
Raleigh, NC

Matthew Bryant
North Carolina State University
Raleigh, NC

ABSTRACT

This paper investigates the effect of resistive forces within a variable recruitment (VR) bundle actuators during recruitment state transition. Due to their versatility in design, ease of manufacturing, high force-to-weight ratio, and inherent compliance, FAMs have become a favorable actuation method for the robotics research community. Recently, researchers have adapted mammalian muscle topology to construct a multi-chamber FAM bundle actuator, consisting of separate units of actuation called motor units (MUs). These bundle actuators have VR functionality in which one or more MUs are sequentially activated according to the load demand. This activation scheme has been shown to have higher actuator efficiencies as compared to a single equivalent cross-sectional area FAM actuator. A characteristic behavior of VR bundles is the interaction between FAM elements in the bundle. Distinctively during recruitment state transition, inactive/low-pressure FAMs buckle outward and are compressed past its free strain due to the higher strain of fully active FAMs. There exists an onset pressure above which such FAMs need to contribute positively to the overall force output of the bundle. This paper presents a realistic scenario in which MU pressure is controlled by a hydraulic servo valve. As a result, the overall bundle force exhibits a sharp decrease during recruitment state transition while the MU being recruited is below the onset pressure.

Keywords: Fluidic artificial muscle, variable recruitment, resistive force

1. INTRODUCTION

Fluidic artificial muscles (FAMs) are soft actuators with high force-to-weight ratios. Due to its compliant nature and contractile motion, it is often compared to biological muscles and have been studied for biomimetic applications. FAMs are simple in design and easily scalable. They consist of an inner elastic bladder that is sheathed by an outer braided mesh. One end of the bladder is closed off while the other end is used to supply pressure, either hydraulically or pneumatically, to activate the FAM. Upon pressurization, the bladder volume changes according to the kinematic constraint imposed by the braided mesh and thus expanding radially and contracting axially.

FAMs are also versatile in design. The braided mesh can be modified using inextensible layers to create bending or torsional actuators. Changing the initial fiber angle of the braided mesh can control the amount of total strain or create extensile actuators. Other studies have grouped together multiple FAMs to be used as a single actuator instead of using single FAMs as stand-alone actuators. A variable recruitment (VR) FAM bundle takes inspiration from how an organic muscle organ is composed of multiple motor units (MUs) that are sequentially activated to adapt to its load demand [[1],[2]]. In a VR bundle, multiple FAMs are connected in parallel by two rigid end plates. One or a group of FAMs are designated as MUs and act as separate units of actuation. Depending on which MUs are active, the VR bundle is said to be operating at a certain recruitment state. Compared to a single FAM without variable recruitment functionality that has equivalent blocked force and free strain conditions, a VR bundle has been proven have higher overall efficiencies. Other studies have investigated the control of the overall force and strain outputs of the bundle [1],[3].

Studies have investigated the control of a VR bundles using model-based feedforward control in which bundle force and strain output is controlled based on determination of the individual MU pressures requirements [4],[5]. In doing so, the modeling of the overall force-strain space of a variable recruitment bundle is determined by the modeling of individual FAMs. A recent model by Kim et al. was proposed specifically for the purpose of characterizing FAMs within a variable recruitment bundle [6]. In typical applications, only the force generation of FAMs up to free strain is of interest. However, in a

variable recruitment bundle in which FAMs are activated sequentially, FAMs are compressed past its free strain, exerting a *resistive force* that hinders the overall force output of the bundle.

The purpose of this study is to investigate the control implications during recruitment state transition when using the resistive force FAM model in characterizing the force-strain space of a two-MU variable recruitment bundle. According to the generated bundle force-strain space, the pressures of each MU required to produce sinusoidal contraction of the bundle are presented. Additionally, pressure dynamics are modeled via a hydraulic servo valve to present a realistic pressure control scenario to demonstrate the effect of resistive force on the overall force output of the VR bundle.

2. RESISTIVE FORCE MODELING

A quasi-static force model was derived by Chou and Hannaford using a balance between the virtual work done by the equilibrium force in the axial direction F and the internal pressure P, which can be expressed as,

$$-F_{mesh}\delta l = P\delta V \tag{1}$$

where δl is the variation of the FAM length and δV is the variation of bladder inner volume [7]. A kinematic relationship between the FAM length and radius is derived as a function of the initial braid angle α_0. The instantaneous radius r can be expressed as,

$$r = r_0\left(\frac{\sqrt{1-cos^2\alpha_0(l/l_0)^2}}{sin\alpha_0}\right) \tag{2}$$

where r_0 is the initial radius, l_0 is the initial length and l is the instantaneous length. The force output of the FAM in the axial direction is expressed in terms of applied internal pressure and the instantaneous strain ε of the FAM.

$$F_{mesh} = \pi r_0^2 P\left(\frac{1}{tan^2\alpha_0}(\varepsilon-1)^2 - \frac{1}{sin^2\alpha_0}\right) \tag{3}$$

This force is often referred to as the *ideal* or *mesh* force as it expresses the axial force due to the volume change of the pressurized bladder imposed by the kinematic constraint of the braided mesh. Comparison of experimental force-strain data to the mesh force model tends to overpredict both force and strain. However, this model serves as a fundamental base upon which other effects such as bladder wall thickness, friction between mesh and bladder, and tapered-end geometry of the bladder can be modeled into [8]. Among such effects, the nonlinear elasticity of the bladder has been model by Klute and Hannaford using the Mooney-Rivlin strain energy function W [9]. In this model, the total force is the sum of the force due to the mesh and the force of the bladder.

$$F_{total} = F_{mesh} + F_{bladder} = P\frac{dV}{dL} - V_b\frac{dW}{dL} \tag{4}$$

The force due the bladder $F_{bladder}$ is negative and thus opposes the force generation of the FAM in the tensile region. Inclusion of the bladder force explains the pressure-dependent free strain behavior of FAMs that can be observed from their force-strain experiments.

A recent model by Kim et al. builds upon the Klute and Hannaford model to characterize FAM behavior past its free strain [6]. Forces beyond free strain can be calculated using previous models assuming the FAM deforms axisymmetrically. However, any imperfections in the FAM or misalignment in its assembly will cause it to buckle outward as it is compressed past free strain. In this compressive strain region, the FAM force is negative. In the context of a variable recruitment bundle, inactive or low-pressure FAMs are compressed beyond free strain and buckle outwards due to the higher strain value of fully active ones. Consequently, those FAMs exert *resistive forces* opposing that of active ones. Based on physical observation of FAMs in the compressive region, the resistive force is divided into two regions: post-buckled and post-collapsed regions. The post-buckled region begins immediately after free strain and the axial force exert by the FAM is derived using a virtual work balance between the potential energy stored in the buckled bladder and the equilibrium force F_b, in the axial direction. The resulting force in the post-buckled region is expressed as

$$F_{total} = F'_{mesh} + F_{bladder}(\varepsilon_{free}) + F_b \tag{5}$$

where F'_{mesh} is the braided mesh force using the arc length of the FAM in its buckled shape and ε_{free} is the free strain. The FAM is in the post-buckled region until it is compressed further, and the internal moment generated along the FAM reaches a critical strain, at which the FAM collapses and folds upon itself. The FAM force in the post-collapsed region is expressed as,

$$F_{total} = F_c + (F_b - F_c)^{-\beta(\varepsilon-\varepsilon_c)} \tag{6}$$

where F_c is the axial force of the bladder in its collapsed shape and ε_c is the strain at collapse. The detailed derivation of this model is presented in the study by Kim et al. [6]. FIGURE 1 illustrates the constant pressure force-strain curve of a FAM in the tensile, post-buckled and post-collapsed regions.

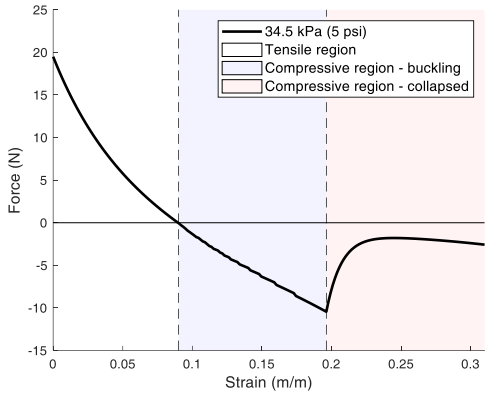

FIGURE 1: FORCE VERSUS STRAIN CURVE OF A FLUIDIC ARTIFICIAL MUSCLE (FAM) IN THE TENSILE (WHITE), POST-BUCKLED (BLUE) AND POST-COLLAPSED (RED) REGIONS. THE FAM USED TO GENERATE THIS PLOT HAS AN INITIAL LENGTH OF 0.1 m, INITIAL OUTER RADIUS OF 0.006 m, BLADDER THICKNESS OF 0.001 m AND AN INITIAL BRAID ANGLE OF 33°.

3. VARIABLE RECRUITMENT BUNDLE FORCE-STRAIN SPACE

The resistive force FAM model can be used to generate the force-strain space of a VR bundle with two recruitment states, which is shown in FIGURE 2. The recruitment state of a VR bundle is determined by the activation of MUs. In recruitment state 1, only MU1 is activated. In recruitment state 2, MU1 and MU2 are activated. In the second recruitment state, MU1 remains activated at its maximum pressure (fully active) while MU2 pressure may vary. Each MU consists of a single FAM with identical dimensions as the one used to generate the curve in FIGURE 1. The constant pressure force-strain curves are plotted at an interval of 34.5 kPa (5 psi) from 0 kPa to 344.7 kPa (50 psi). Thicker line widths are used to indicate higher pressures.

The implication of resistive forces on the bundle overall force and strain output is illustrated by an overlapping region between recruitment states 1 and 2. When MU1 is at its maximum pressure, any additional force or strain required necessitates the activation of MU2. However, an initial increase in MU2 pressure results in a decrease in force or strain output as indicated by the overlapping region. This is due to the resistive force of MU2 that act against the fully activated force output of MU1. Thus, there exists a minimum pressure of MU2 during recruitment state transition that is required for MU2 to contribute positively to the overall force or strain output of the bundle. This pressure will hereon be referred to as *onset pressure*.

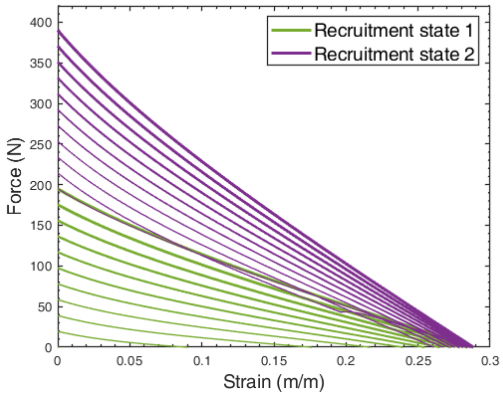

FIGURE 2: FORCE-STRAIN SPACE OF A VARIABLE RECRUITMENT (VR) BUNDLE WITH TWO RECRUITMENT STATES. AN OVERLAPPING REGION EXISTS DUE TO RESISTIVE FORCES.

FIGURE 3 shows the theoretical force contribution of MU2 to the overall force of the bundle determined using the resistive force FAM model. During recruitment state transition, the MU being recruited initially is a zero pressure, at which the MU exerts a non-zero resistive force due to the deformation of the bladder. In the physical system, MU2 is in the buckled state. The magnitude of resistive force initially increases as applied pressure increases. MU2 gradually becomes less buckled as the applied pressure reaches the onset pressure at which the free strain of MU2 equals the bundle strain. At this pressure, MU2 is contributing neither negative nor positive force. Because the force at which MU1 is dependent on strain, the onset pressure is also strain-dependent as shown by FIGURE 3.

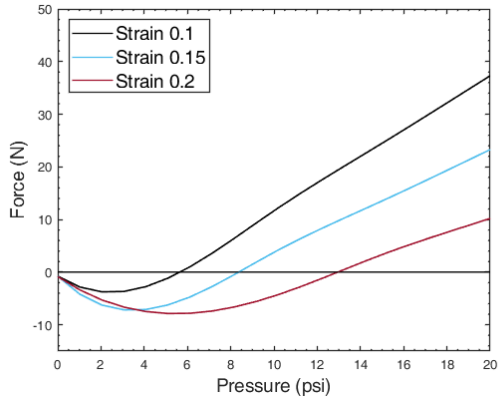

FIGURE 3: FORCE CONTRIBUTION OF MU2 TO THE OVERALL BUNDLE FOR DIFFERENT BUNDLE STRAINS SHOWING THE STRAIN-DEPENDENCE OF ONSET PRESSURE.

4. IMPLICATIONS OF ONSET PRESSURE ON BUNDLE FORCE OUTPUT

The presence of an overlapping region in the bundle force-strain space and a resulting onset pressure has implications on the control of bundle output. Let us consider a case in which the strain remains constant and the force profile is prescribed as a spline, shown in **FIGURE *4***. A constant strain of 0.2 and a force

profile, beginning at 0 N and increasing up 100 N, is chosen as to demonstrate the effect of onset pressure during recruitment state transition.

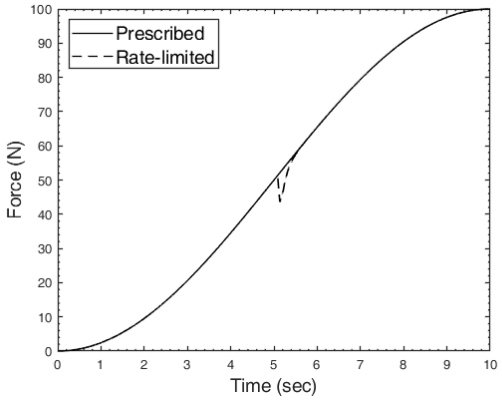

FIGURE 4: PRESCRIBED FORCE PROFILE FOR A VARIABLE RECRUITMENT (VR) BUNDLE AT CONSTANT STRAIN OF 0.2 (SOLID). IN A REALISTIC CASE IN WHICH PRESSURE INCREASE RATE IS LIMITED, RESISTIVE FORCES CAUSE A SHARP DECREASE IN FORCE (DASHED).

The force-strain space for a VR bundle presented in FIGURE 2 is used to generate the required pressures for MU1 and MU2 as shown by solid lines in FIGURE 5.

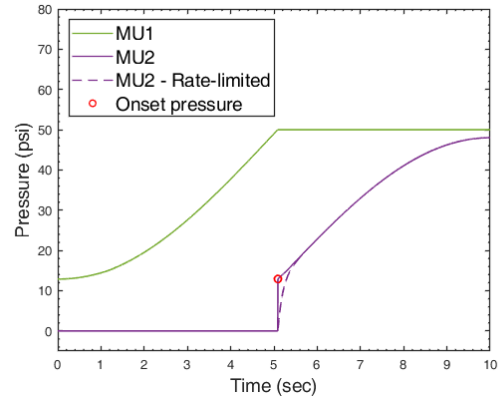

FIGURE 5: MOTOR UNIT (MU) 1 AND MU2 PRESSURES REQUIRED TO PERFECTLY TRACK THE FORCE PROFILE IN FIGURE 4. THE RATE-LIMITED CASE INCLUDING PRESSURE DYNAMICS IS SHOWN BY THE DASHED LINE.

As the required force increases, the pressure of MU1 increases until it reaches the source pressure set at 50 psi. No additional force can be generated with only MU1 and thus the second MU is activated. For the second MU to add force to the overall force output of the bundle, the applied pressure to MU2 must be at least equal to the onset pressure. The onset pressure is indicted with a red marker in FIGURE 5 which is in accordance with the pressure at which force becomes positive for the 0.2 strain case in FIGURE 3. However, it should be noted that an instantaneous 'jump' from zero to the onset pressure is impossible to realize. In a realistic system that includes pressure transients, the rate of pressure increase would be limited by the hydraulic circuit components such as the hydraulic servo valve or motor/pump assembly. To demonstrate the effects of introducing pressure transients during the control of MU1 and MU2 pressure, the flow dynamics of a hydraulic servo valve is presented [10]. The flowrate into a MU is expressed as:

$$Q_v = c_v d_v sgn(P_{acc} - P_{app})\sqrt{|P_{acc} - P_{app}|} \tag{7}$$

where d_v is the port diameter, P_{acc} is the accumulator pressure and P_{app} is the MU applied pressure. The flow coefficient, c_v, is calculated using the nominal flowrate, Q_N, and nominal pressure drop, Δp_N, across the maximum port diameter, $d_{v,max}$.

$$c_v = \frac{Q_N}{\sqrt{\Delta p_N/2}\cdot d_{v,max}} \tag{8}$$

The inflow of fluid into a MU as governed by Equation (1) is used to determine its pressure dynamics. The MU force and strain is determined by the pressure as a result of compression of MU internal fluid. The pressure dynamics of the MUs are expressed as below:

$$\frac{dP}{dt} = \frac{1}{\beta}\frac{Q - \dot{V}_{MU}}{V_{MU}} \tag{9}$$

where β is the compressibility of fluid and V_{MU} is the MU internal fluid volume. The parameters used for the pressure dynamics are summarized in Table 1 [11].

TABLE 1: HYDRAULIC SERVO VALVE PARAMETERS

Nominal flowrate (l/m)	Q_N	63
Nominal pressure drop (kPa)	Δp_N	350
Max. port diameter (m)	$d_{v,max}$	0.001
Hydraulic oil compressibility (kPa)	$1/\beta$	2.15×10^6

The rate-limit does not affect MU1 pressure as its rate of change is slower. However, MU2 pressure requires an instantaneous increase to the onset pressure at which the fluid flowrate and pressure increase rate are restricted by the valve. The rate-limited pressure of MU2, according to the servo valve dynamic equations, is shown as a dashed line in FIGURE 5. The rate-limited case depicts a more realistic scenario in which a model-based feedforward controller is implemented to control the bundle force. The dashed force curve in FIGURE 4 shows the overall bundle force output when determined by the rate-limited pressures of MU1 and MU2. Note that as MU2 begins to activate, the applied pressure remains below the onset pressure at which the force output is negative, i.e. exerting a resistive force that opposes the force of MU1. Due to this negative force contribution, the overall force output of the bundle sharply

decreases, deviating from the intended force output. Although it is possible to decrease the time during which MU2 exerts this negative force by increasing the response speed of the system, it is impossible to eliminate the drop entirely or decrease the magnitude of force drop. Therefore, a comprehensive study based on the resistive force model is required to devise a recruitment state transition strategy that overcomes such undesired effects.

5. CONCLUSION

This study investigates the effect of resistive forces in a VR FAM bundle and its implication on the overall bundle force output in a realistic scenario that includes servo valve dynamics. During transition from recruitment state 1 to recruitment state 2, there exists a minimum MU2 onset pressure at which its force contribution becomes positive. At any pressures below the onset pressure, the difference in strain between MU1 and MU2 causes MU2 to buckle outward, exerting a resistive force that lowers the force output of the bundle. The resistive force model gives us a physics-based understanding of the effects of MU behavior during recruitment state transition, upon which further studies can build toward developing an effective transition strategy.

ACKNOWLEDGEMENTS

This work was supported primarily by the Faculty Early Career Development Program (CAREER) of the National Science Foundation under NSF Award Number 1845203 and Program Manager Irina Dolinskaya.

REFERENCES

[1] Bryant, M.; Meller, M. A.; Garcia, E. Variable Recruitment Fluidic Artificial Muscles: Modeling and Experiments. 2014, 23, 74009. 10.1088/0964-1726/23/7/074009

[2] R. M. Robinson; C. S. Kothera; N. M. Wereley. Variable Recruitment Testing of Pneumatic Artificial Muscles for Robotic Manipulators. IEEE/ASME Transactions on Mechatronics 2015, 20, 1642-1652. 10.1109/TMECH.2014.2341660

[3] Meller, M.; Chipka, J.; Volkov, A.; Bryant, M.; Garcia, E. Improving actuation efficiency through variable recruitment hydraulic McKibben muscles: modeling, orderly recruitment control, and experiments. Bioinspir. Biomim. 2016, 11, 065004. 10.1088/1748-3190/11/6/065004

[4] Meller, M.; Kogan, B.; Bryant, M.; Garcia, E. Model-based feedforward and cascade control of hydraulic McKibben muscles. Sens. Actuator A Phys. 2018, 275, 88-98. 10.1016/j.sna.2018.03.036.

[5] Jenkins, T. E.; Chapman, E. M.; Bryant, M. Bio-inspired online variable recruitment control of fluidic artificial muscles. Smart Mater. Struct. 2016, 25, 125016. 10.1088/0964-1726/25/12/125016.

[6] Kim, J. Y.; Mazzoleni, N.; Bryant, M. Modeling of Resistive Forces and Buckling Behavior in Variable Recruitment Fluidic Artificial Muscle Bundles. Actuators. 2021, 10, 42. 10.3390/act10030042.

[7] Chou, C.; Hannaford, B. Measurement and Modeling of McKibben Pneumatic Artificial Muscles. IEEE Trans. Robot. Autom. 1996, 12, 90-102. 10.1109/70.481753.

[8] Tondu, B.; Lopez, P. Modeling and Control of McKibben Artificial Muscle Robot Actuators. IEEE Control Systems Magazine. 2000, 20, 15-38. 10.1109/37.833638.

[9] Klute, G.; Hannaford, B. Accounting for Elastic Energy Storage in McKibben Artificial Muscle Actuators. ASME. J. Dyn. Syst. Meas. Control. 2000, 122, 386-388. 10.1115/1.482478.

[10] Vemula, D.; Kim, J. Y.; Mazzoleni, N.; Bryant, M. Design, analysis, and validation of an orderly recruitment valve for bio-inspired fluidic artificial muscles. Bioinspir. Biomim. 2021, 17, 026001. 10.1088/1748-3190/ac4381.

[11] Jelali, M.; Kroll, A. Hydraulic servo-systems: modelling, identification and control. Springer Sciences & Business Media. 2012.

